Phase-Shift-Keying (PSK & DPSK) Techniques for Long-Haul Wavelength-Division-Multiplexing Systems over Standard Single-Mode Fiber

Jochen Leibrich*, Christoph Wree, Werner Rosenkranz
Chair for Communications, University of Kiel, Germany

ABSTRACT

In order to increase the transmittable data rate and to enlarge the transmission distance, the spacing between WDM channels has to be decreased while the optical transparent length must be increased both giving rise to interchannel crosstalk induced by fiber nonlinearities like cross-phase modulation (XPM). Thus, the development of modulation techniques being robust towards these effects is necessary. Recently, phase shift keying (PSK) techniques have attracted remarkable interest. For PSK-techniques, the optical power as a function of time is approximately constant (for non-return-to-zero (NRZ) signaling) or periodic (for return-to-zero (RZ) signaling). This is an advantageous property for the reduction of nonlinear phase modulation (PM) induced by the effect of XPM. On the other hand, since for PSK-techniques the information is carried by the phase of the optical carrier, the sensitivity to the nonlinear PM is high. In our contribution, we present an analytical model for the XPM-induced PM. With the help of this model and the visualization of XPM in the complex plane, we prove that the differential self-homodyne implementation of PSK is robust towards the nonlinear PM while PSK-techniques using a local oscillator in the receiver are extremely sensitive.

Keywords: Optical communication, nonlinear effects, cross-phase modulation, modulation formats, phase-shift keying, long-haul, analytical modeling

1 INTRODUCTION

Recently, there have been remarkable changes considering the focus of world-record lab experiments. Up to the year 2000, every year the amount of data that was transmitted over a single fiber was approximately doubled, yielding data rates beyond 10Tb/s over at most some hundreds of kilometers[1,2]. However, since last year the distance that is bridged using these high data rates becomes more and more of interest reaching a product of capacity times distance of 10Pb/s · km (2.5Tb/s over 4000km) [3].

For the transmission over relatively short distances the on-off keying (OOK) technique (also known as amplitude-shift keying (ASK)) was a suitable modulation format because of its relatively easy feasibility compared to other modulation formats. However, for long-haul transmission the interaction length between adjacent channels is large giving rise to nonlinear effects. Thus, modulation techniques that are robust towards these nonlinear effects now have become the key issue for long-haul Tb/s transmission. This becomes evident when noticing, that the experiment carried out in [3] has been performed using a differential phase shift keying technique in conjunction with RZ-pulse shaping that has also been proposed in several publications[4,5,6] where the robustness towards nonlinear effects has been shown experimentally[5] and theoretically[6].

Following latest developments concerning optical modulation formats, PSK techniques have become attracting attention, first as two-symbol transmission. Nevertheless, this year also optical differential QPSK-transmission has been reported[7,8] enabling to double the data rate using the same bandwidth.

Restricting to the two-symbol case, two possible implementations can be found most frequently in the literature: The coherent homodyne PSK implementation using a local oscillator for demodulation[9], and the self-homodyne DPSK

* jol@tf.uni-kiel.de ; phone +49 431 8806165; fax +49 431 8806303; http://www.tf.uni-kiel.de/etech/NT/uk/mitarbeiter/leibrich.html
University of Kiel, Faculty of Engineering, Chair for Communications, Kaiserstrasse 2, D-24143 Kiel, Germany

(=differential PSK) implementation using an optical delay-and-add demodulator[10]. Concerning receiver sensitivity, the coherent PSK implementation is favorable, since the incoming noisy signal is mixed with a (noiseless) signal coming from the local oscillator in contrast to the case where the delay-and-add demodulator is used, where both signals are noisy. This gives an improvement of up to 3dB, depending on the BER[11].

In this paper, we restrict to the case where only a single-pin detector is used. Finally, it has to be noted, that the effort for PSK is much larger, since carrier recovery is required.

For long-haul transmission, there are always two limiting impairments: For low launch powers, the system is limited by noise, while for high launch powers, nonlinear effects give rise to strong signal degradation which can close the eye severely. Thus, receiver sensitivity is not the only criterion for the judgement of a modulation format. Moreover, since the nonlinear Kerr effect acts on the phase of the signal, at first sight PSK techniques seem to be much more sensitive compared to ASK-techniques which only evaluate the envelope of the signal, although the complex envelope of a PSK-signal (more or less constant for NRZ-pulses[9], periodic for RZ-pulses[6]) is known to reduce the induced PM compared to ASK. This may result in an acceptable launch power which is so low, that this cannot be compensated for by the improved receiver sensitivity of this modulation format.

In this paper, we investigate the sensitivity of both coherent PSK and self-homodyne DPSK transmission, which are introduced in section 2, on cross-phase modulation (XPM). This effect turns out to be the limiting impairment for WDM-systems with a data rate of 10Gb/s/channel and channel spacing of at least 50GHz over standard single-mode fiber. In section 3, we develop an analytical model for XPM-induced PM, which provides detailed information about the spectral properties of the induced PM. With the help of this, we show theoretically (section 3) and by simulation (section 4), that the specific demodulation technique using the delay-and-add demodulator makes self-homodyne DPSK transmission very robust towards XPM, while coherent PSK transmission shows extreme sensitivity as presumed above.

2 PHASE-SHIFT-KEYING TECHNIQUES

2.1 PSK: From classical to optical communications

Fig. 2.1 shows a sketch of modulator and demodulator for a bandpass transmission system with carrier frequency f_T. If we assume, that $x(t)$ is a digital baseband signal with

$$x(t) = \sum_{-\infty}^{\infty} b_k \, g(t - kT_b), \tag{2.1}$$

where T_b is the bit rate, $g(t)$ is the impulse response of the pulse former and the data $b_k \in \{-1;1\}$, the transmission scheme is 2-PSK with carrier phases ‘0’ and ‘p’.

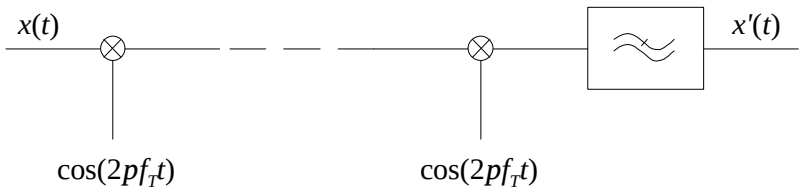

Fig. 2.1: Schematic diagram of bandpass transmission

If we neglect the impact of the transmission channel, we find that $s'(t)=0.5 \cdot s(t)$. As a precondition, the demodulator carrier must be synchronized exactly to the incoming signal and the low pass filter must filter out the signal component occurring at twice the carrier frequency.

Unfortunately, without modifications this schematic is not transferable to optical communications. This is due to the fact, that the optical/electrical conversion done by the photodiode automatically provides a magnitude square operation on the complex envelope of the incoming optical signal. Therefore, for phase-sensitive demodulation of optical signals, the optical carrier is added to the optical signal and then mixed in the photodiode (see fig. 2.2 for coherent PSK and fig. 2.4 for self-homodyne DPSK).

Thus, the demodulation of optical PSK-modulated signals can be interpreted in two different ways: Either as addition of the carrier to the optical bandpass signal followed by a mixing operation in the photodiode (which gives in addition two constant terms where optical signal and local carrier mix with itself, respectively). Or as superposition of the complex envelope of the local carrier (which for ideal carrier recovery is a constant vector in the complex plane) with the complex envelope of the incoming optical signal followed by an evaluation of the squared length of the resulting complex vector. For investigating the influence of XPM on the transmission, we make use of the latter strategy, which is explained more in detail in the following subsections.

2.2 Implementation of optical PSK

Fig. 2.2 depicts a setup for optical PSK-transmission. By proper setting of the bias, the Mach-Zehnder modulator (MZM) produces an optical signal which is PSK-modulated with phases '0' and 'p' (which equals the symbols '+1' and '-1', that originate from the bits '1' and '0', respectively)[12]. The MZM is driven in push-pull configuration. As a consequence, the envelope is not constant during symbol transitions but goes down to zero. This disadvantage is acceptable compared to the high sensitivity towards fiber dispersion of the implementation using a phase modulator, which is caused by the chirp that is introduced during symbol transitions[6].

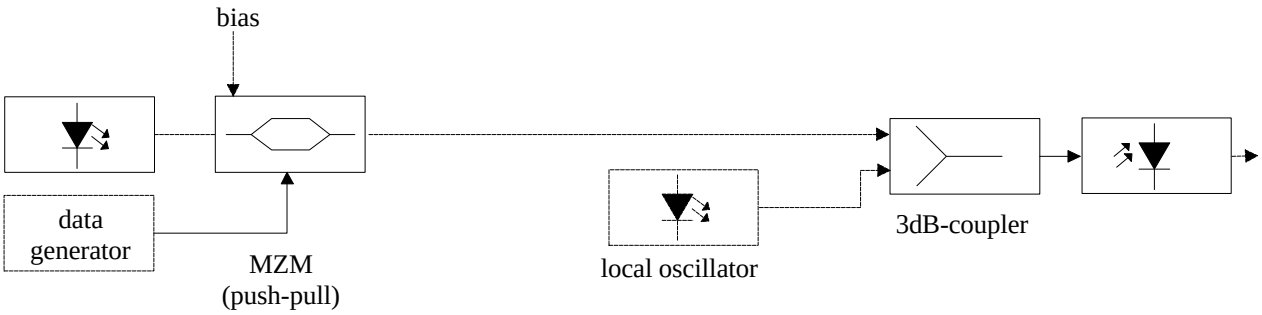

Fig. 2.2: Schematic of optical PSK transmission

The signal processing in the demodulator is clarified in fig. 2.3 a) – c) . Fig. 2.3 a) shows the signal constellation in the complex plane after the MZM. Again neglecting the influence of the channel, the same signal is obtained at the upper input of the 3dB-coupler.

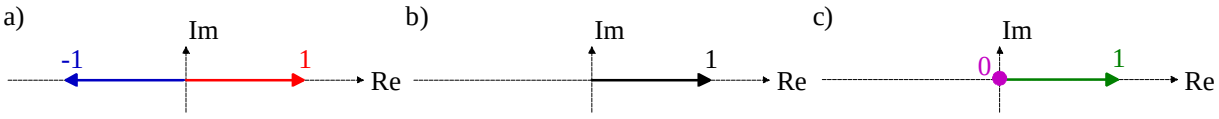

Fig 2.3: Complex vectors of optical signal constellation in the demodulator for PSK-modulation. a) upper input of coupler (=demodulator input), b) lower input of coupler (=local oscillator), c) output of coupler (= sum of a) and b), divided by 2)

Under the assumption of perfect carrier recovery, the local oscillator is synchronized to the '+1'-symbol (fig. 2.3 b)). After addition (and division by 2) in the coupler, for the symbols '+1' and '-1' vectors of length '1' and '0' are obtained, respectively, allowing direct detection of the resulting optical signal (fig. 2.3 c)).

2.3 Implementation of optical DPSK

In contrast to PSK, for DPSK the demodulation is possible without the requirement of using a local oscillator. Instead of the LO-signal, the incoming signal is mixed with a delayed replica of itself, which results in a self-homodyne differential demodulation. In order to avoid error propagation in the receiver when decoding, the data is differentially precoded in the transmitter using a device presented in [13].

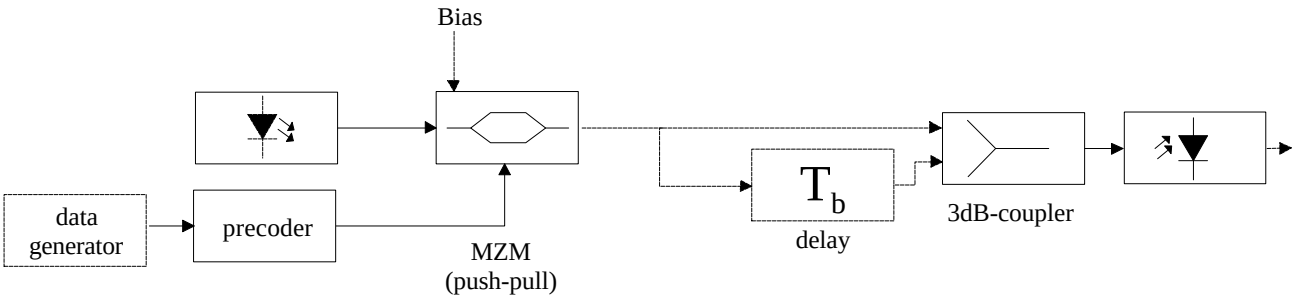

Fig. 2.4: Schematic of optical DPSK transmission

As a result, a '0' is coded as symbol change, while for a '1' the same symbol is transmitted. The decoding is depicted in fig. 2.5 a) – c). Figs 2.5 a) and 2.5 b) show the demodulator input and the delayed input, respectively. Both of the signals can take the symbols '+1' and '-1', respectively. After the coupler, for the case that two consecutive symbols are equal, the resulting complex vector has a phase shift of '0' or '*p*' but length '1', so that taking the squared length a '1' bit is obtained. On the other hand, for a symbol transition the complex vectors add up to null (fig. 2.5 c)).

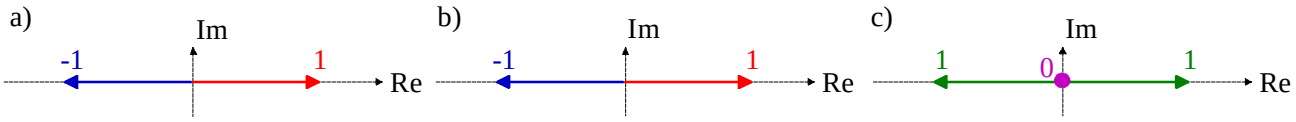

Fig 2.5: Complex vectors of optical signal constellation in the demodulator for DPSK-modulation. a) upper input of coupler (=demodulator input), b) lower input of coupler (=delayed demodulator input), c) output of coupler (= sum of a) and b), divided by 2)

3 INFLUENCE OF CROSS-PHASE MODULATION ON PSK/DPSK-TRANSMISSION

3.1 Basic properties of XPM

For single channel systems, the Kerr effect results in the modulation of the phase of the transmitted signal by the signal itself, also known as self-phase modulation (SPM). Making the step towards multi-channel systems gives rise to intermodulation products, like for every multi-channel transmission passing nonlinear elements. Depending on whether these intermodulation products automatically fall onto the generating channels or not, they are separated into cross-phase modulation (XPM) or four-wave mixing (FWM).

The properties of SPM, XPM and FWM are complex and fairly different from each other. Thus, although all of them originate from the Kerr effect it is reasonable to create a theoretical framework for each of the effects individually. In this paper, from now on we restrict to XPM.

For equal input power levels of the WDM-channels due to XPM all the channels interact pairwise to the same extent. Nevertheless, for the analytical analysis we consider a pump-probe situation where we investigate the influence of one disturbing (pump) channel onto another disturbed (probe) channel.

As we will see in a more detailed form in the subsequent subsection, due to XPM the optical power of the pump channel introduces a PM onto the probe channel. This is to some extent similar to SPM, where the optical power of one channel modulates the phase of the channel itself. However, the important difference between SPM and XPM can be explained as follows:

Due to fiber dispersion the WDM-channels travel at different group velocities, also known as walk-off [14]. Thus, while for SPM the PM is correlated with the signal shape (i.e. the phase shift is maximum for high power components of the optical signal and minimum for low power components), for XPM this is not the case. Moreover, the larger the channel spacing between pump and probe channel, the larger the group velocity difference between them. A large group velocity difference results in an averaging of the induced PM. Thus, only the low frequency components of the pump channel cause significant PM in the probe channel, and the larger the channel spacing the lower the cut-off frequency for this process. This will be derived analytically in subsection 3.3.

For phase-modulated transmission, impairments inducing phase disturbance are very crucial. However, we will see that the spectral properties of the induced PM in conjunction with the delay-and-add demodulator for DPSK-transmission introduced in the previous section result in almost negligible influence of the induced PM while for the case of PSK-transmission using a local oscillator significant eye-closure is obtained.

For direct detection disturbing PM does not affect the transmission performance of the system, since for direct detection the phase information is lost. However, in the presence of dispersion the PM is converted into intensity modulation [15], which can be modeled as an additive noise on the optical intensity (i.e. on the photo current after direct detection). This intensity modulation affects the performance of both phase modulated and intensity modulated signals, but will not be discussed throughout this paper in detail.

This section is organized as follows: First the nonlinear Schrödinger equation is introduced as a basis for modeling nonlinear signal propagation. Thereafter, the spectral properties of the induced PM in dependence of the channel spacing are derived. Finally, the impact of XPM on the complex envelope is depicted in the complex plane and the robustness of self-homodyne DPSK in contrast to coherent PSK is clarified.

3.2 Representation of XPM using coupled Schrödinger equations

The propagation of the complex envelope $A(z,t)$ of an optical signal along a nonlinear optical fiber is given by the well-known nonlinear Schrödinger equation (NLSE)[16]:

$$\frac{\partial A(z,t)}{\partial z}+\frac{a}{2}A(z,t)-\frac{j}{2}b_2\frac{\partial^2 A(z,t)}{\partial t^2}-\frac{1}{6}b_3\frac{\partial^3 A(z,t)}{\partial t^3}=-jg\left|A(z,t)\right|^2 A(z,t), \tag{3.1}$$

where z is the spatial coordinate, a accounts for fiber loss, b_2 and b_3 represent fiber dispersion, and g is the nonlinear Kerr coefficient. For single-channel transmission, eq. (3.1) takes into account loss, dispersion and SPM.

However, for the propagation of an optical WDM-signal the coupled nonlinear Schrödinger equations[16] can be used. Here, for each of the N channels one equation is provided:

$$\frac{\partial A_i}{\partial z}+\frac{a}{2}A_i+b_{1i}\frac{\partial A_i}{\partial t}-\frac{j}{2}b_{2i}\frac{\partial^2 A_i}{\partial t^2}-\frac{1}{6}b_{3i}\frac{\partial^3 A_i}{\partial t^3}=-jg_i\left(\left|A_i\right|^2+2\sum_{\substack{k\\k\neq i}}\left|A_k\right|^2\right)A_i-jg_i\sum_{\substack{i=p+q-r\\p,q\neq r}}\tfrac{d}{3}A_pA_qA_r^*e^{j\Delta b_{ipqr}z} \tag{3.2}$$

On the right hand side of eq. (3.2), in addition to the SPM-contribution already included in eq. (3.1), XPM and FWM are represented by coupling terms, where d and Db_{pqr} are the FWM degeneracy factor and the phase mismatch, respectively[17].

We now consider WDM transmission systems, which are XPM-limited. This is the case e.g. for data rates of 10Gb/s and channel spacings of at least 50GHz on standard single mode fiber. Due to this fact, we can omit the coupling terms representing FWM. Moreover, for the analytical investigation, we restrict to the 2-channel case and introduce a reference frame moving synchronously with channel 1, yielding the neglect of the group delay in channel 1 and the representation of the dispersion-induced channel walk-off of by $d_{12}=D(\lambda_1-\lambda_2)$, where D is the dispersion coefficient, and λ_i is the carrier wavelength of channel i.

From now on, we will investigate the influence of channel 2 (disturbing pump channel) on channel 1 (disturbed probe channel).

3.3 Modeling XPM-induced phase modulation

We assume, that the complex envelope change due to dispersion does not affect the PM induced by XPM. Thus, we neglect b_{2i} and b_{3i}, i=1,2, yielding

$$\begin{aligned} \frac{\partial A_1}{\partial z}+\frac{\alpha}{2}A_1 &= -j\gamma_1\left(|A_1|^2+2|A_2|^2\right)A_1 \\ \frac{\partial A_2}{\partial z}+\frac{\alpha}{2}A_2-d_{12}\frac{\partial A_2}{\partial t} &= -j\gamma_2\left(|A_2|^2+2|A_1|^2\right)A_2 \end{aligned} \tag{3.3}$$

Moreover, the influence of the pump envelope change (A_2) due to nonlinearity on the PM induced in the probe channel is neglected, too, which gives

$$A_2(z,t)=A_2(0,t+d_{12}z)e^{-\frac{\alpha}{2}z}. \tag{3.4}$$

Since for insertion into the upper equation of (3.3) we need the magnitude square of A_2, we find

$$|A_2(z,t)|^2=P_2(z,t)=|A_2(0,t+d_{12}z)|^2e^{-\alpha z}=P_2(0,t+d_{12}z)e^{-\alpha z}, \tag{3.5}$$

where $P_2(t)$ is the optical power of channel 2. Thus, only walk-off and attenuation are considered for the pump channel. This result is inserted into the first equation of (3.3), the solution of which for a fiber of length L reads:

$$A_1(L,t)=A_1(0,t)e^{-\frac{\alpha}{2}L}e^{-j\varphi_{1SPM}(L,t)}e^{-j\varphi_{1XPM}(L,t)} \tag{3.6}$$

where we find the XPM-induced PM as

$$\varphi_{1XPM}(L,t)=2\gamma_1\int_0^L P_2(z,t)\,dz=2\gamma_1\int_0^L P_2(0,t+d_{12}z)e^{-\alpha z}dz. \tag{3.7}$$

The integration can be carried out in the frequency domain very easily:

$$f_{1XPM}(L,f) = P_2(0,f)\,2g_1\int_0^L e^{(j2p\,fd_{12}-a)z}dz \overset{e^{-aL}<<1}{\approx} P_2(0,f)\frac{2g_1}{a-j2p\,fd_{12}} = P_2(0,f)H_{12}(f)\cdot \tag{3.8}$$

From eq. (3.8) we see, that the XPM-induced PM in the probe channel is obtained by passing the optical power of the pump channel through a linear filter, the frequency response of which is a low pass filter of first order with cutoff-frequency

$$f_c = \frac{a}{2p\,d_{12}}\cdot \tag{3.9}$$

For a loss of 0.2 dB/km, dispersion coefficient D=17ps/(nm·km) and a channel spacing of 0.8nm, f_c takes a value of ≈540MHz, which is far below the data rate of 10Gb/s. Thus, this analytical model confirms the qualitative considerations of section 3.1, where we stated, that only the low frequency components of the disturbing channel cause significant PM and the cutoff frequency reduces with increasing channel spacing (i.e. increasing group delay difference).

3.4 XPM in the complex plane

In this subsection, we clarify the influence of XPM-induced PM on (D)PSK-modulated signals. Two our knowledge, this is the first time that this is done in the complex plane allowing deep insight and understanding of the impact of XPM.

First, we separate the power signal $P_2(t)$ of the pump channel into DC-value and zero-mean signal. Since the low pass model given in (3.8) is a linear system, the DC-value is the origin of a mean phase shift, while the time-varying PM stems from the zero-mean time varying portion of $P_2(t)$ (see fig. 3.1).

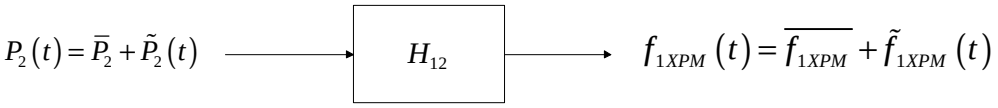

Fig. 3.1: Separation of pump power and phase modulation into DC-value and zero-mean signal

Thus, the signals in the complex plane (see e.g. figs. 2.3 a) and 2.5 a)) experience a clockwise rotation (remember the definition of the PM with negative sign in eq. (3.6)). Because of the time varying component, in addition to the constant rotation the data symbols lose their exact location in the complex plane but are spread over a continuous region on a circle (see fig. 3.2). The instantaneous position depends stochastically on the power in the pump channel. Nevertheless, it is important to mention, that the phase change is slow compared to the data rate, which is a direct consequence of the low pass properties of H_{12}. This means, that for equal consecutive symbols, the location in the complex plane changes only little while for a symbol transition the location being almost exactly at the opposite side with respect to the origin is taken.

In the following two subsections, the impact of this phase change on the photo current after demodulation is investigated for the two different implementations of PSK-modulation presented in subsections 2.2 and 2.3.

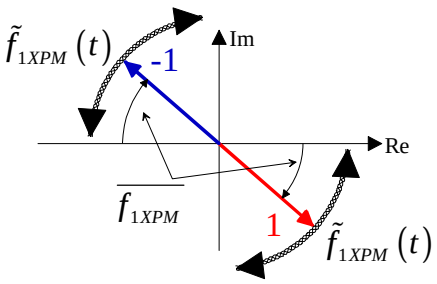

Fig. 3.2: Spreading of transmitted symbols in the complex plane because of XPM-induced phase modulation

3.5 Influence of XPM on PSK-transmission

Although the induced PM is slow compared to the bit rate, it consists of frequency components from DC up to some hundreds of MHz. In order to guarantee sufficient stability, the carrier recovery cannot follow the fast phase change. Therefore, the consideration of a local oscillator synchronized on the mean phase shift is a reasonable approach[9]. Again assuming, that the LO is synchronized to the '+1'-symbol, behind the coupler we find a complex envelope directly in front of the photo diode, which is shown in fig. 3.3.

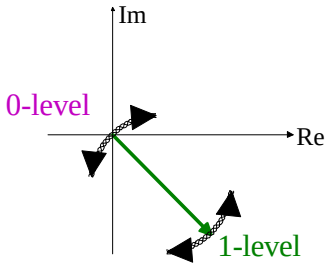

Fig. 3.3: Complex envelope of optical signal in front of the photo diode for PSK-modulation

Evaluating the squared length of the complex vector, we find, that because of XPM the 0-level increases remarkably while on the other hand the 1-level decreases. For strong influence of XPM (which can occur for relatively high powers and high interaction lengths) both levels can merge making a distinction between the symbols impossible.

3.6 Influence of XPM on DPSK-transmission

For self-homodyne DPSK demodulation, the addition in the coupler is done with a replica of the same signal delayed by one bit duration. In subsection 3.4, we already clarified, that because of the slow PM compared to the bit rate for equal consecutive symbols the complex vectors are almost completely parallel. Thus, they add up to a vector having the same phase but double length (which is compensated for by the division by 2). Thus, no decrease of the 1-level is expected, independent of whether the two symbols are of type '+1' or '-1' (see fig 3.4). On the other hand, for a symbol transition, the complex vectors are almost exactly anti-parallel, thus preserving a sharp 0-region after summation.

Therefore, even if the symbols merge because of strong XPM, using the differential demodulator allows direct detection of the signal at demodulator output. The XPM-induced PM only affects the phase of the signal after demodulation, which does not have any influence on the photo current.

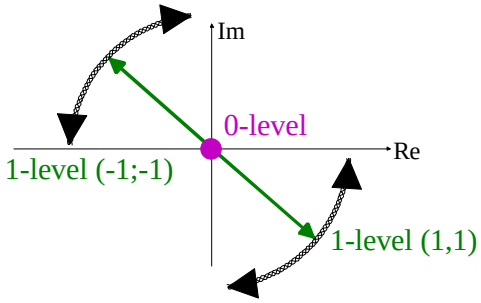

Fig. 3.4: Complex envelope of optical signal in front of the photo diode for DPSK-modulation

4 SIMULATION RESULTS

4.1 System setup

In this section, the theoretical considerations of the previous section are confirmed by simulation. Therefore, we investigate a WDM system of 16 channels with either coherent PSK modulation or self-homodyne DPSK-modulation at a channel spacing of 100GHz. The carrier frequencies are conform to the ITU-grid (193.1THz – 194.6THz). The signals are multiplexed and transmitted over several spans which consist of 100km of standard single mode fiber with a loss of 0.2dB/km, D=17ps(nm·km), n_2=3.2·10^{-20}m^2/W, A_{eff}=80µm^2, a dispersion compensating fiber, which is considered linearly providing 100% post compensation, and an optical amplifier compensating for the total span loss.

We inspect the 8th channel at a carrier frequency of 193.8THz. In order to avoid SPM, the input power for this channel is fixed to 0dBm, while the input powers P_{in} for the remaining 15 channels are varied synchronously from 0 to 15dBm. Thus, the transmission is purely XPM-limited. After the last span, the 8th channel is extracted and demodulated.

For the data signal, we use NRZ pulse shaping and a PRBS-length of 2^{10}-1. In subsection 4.3, the influence of the PRBS-length on the simulation result is investigated.

4.2 Numerical results

Fig. 4.1 shows the eye-opening penalty (EOP) vs. the input powers P_{in} for the disturbing 15 channels for transmission over 100km and 200km, respectively.

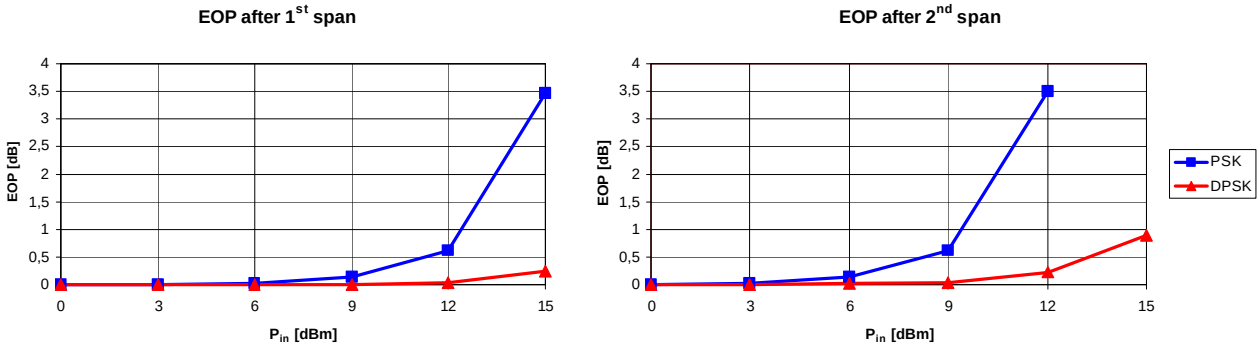

Fig. 4.1: Eye-opening penalty (EOP) vs. fiber input power of the disturbing channels for transmission over one span (left) and two spans (right) for coherent PSK transmission (squares) and self-homodyne DPSK transmission (triangles)

The following conclusions can be drawn:

- For transmission over one span, the eye-opening penalty (EOP) for low values of P_{in} is negligible. For increasing power the eye closure is dramatic for coherent PSK while still very small for self-homodyne DPSK transmission, which confirms the considerations in 3.5 and 3.6.
- For transmission over two spans, the relative situation is the same while significant eye closure is obtained already for lower values for P_{in}.
- Comparing both diagrams, for two-span transmission the same values for the EOP are obtained at exactly half the power compared to single-span transmission. This is reasonable, since the induced PM is proportional to the power as well as to the number of spans (for 100% post compensation[18]).

Using these proportionality, we can predict the relationship of input power vs. number of spans for an EOP of 1dB, which is shown in fig. 4.2. As can be seen, for the same transmission length for self-homodyne DPSK the acceptable input power is approximately 5dB higher compared to coherent PSK, which is well above the more advantageous receiver sensitivity of PSK of at most 3dB (typically 1dB for a BER of 10^{-9} [11]).

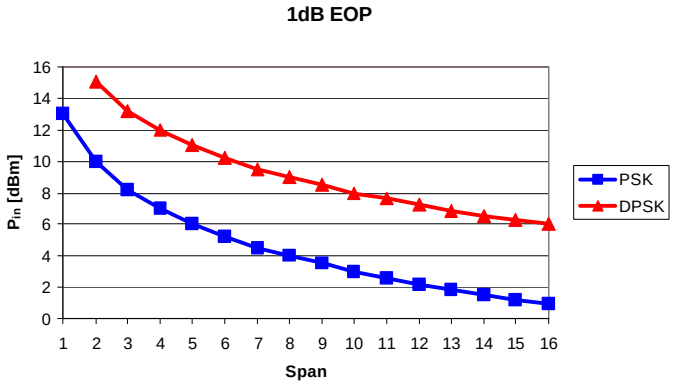

Fig. 4.2: Fiber input power versus transmission length for EOP of 1dB for coherent PSK transmission (squares) and self-homodyne DPSK transmission (triangles)

4.3 Influence of the PRBS-length on the simulation result

For a realistic investigation of the influence of the XPM-induced PM, the periodicity of the considered data signal is a very critical parameter. Because the low frequencies of the disturbing channels are actually the origin of the PM, in the data signal these low frequencies must be represented sufficiently. For example, for the impact of channel 16 on channel 8, the cutoff frequency of the low pass model takes a value of approximately 75MHz. At a data rate of 10Gb/s, for a PRBS-length of 2^7-1, which is a usual value for numerical simulation, the fundamental component takes a value of approximately 80MHz. Thus, from point of view of XPM-induced crosstalk, this signal does not emulate a real data signal sufficiently.

This is confirmed by the results shown in fig. 4.3 for single span transmission at P_{in}=15dBm. For coherent PSK, the EOP grows with increasing PRBS-length, while for self-homodyne DPSK for a length of 2^{10}-1 a saturation is obtained. Thus, the results presented in the previous section are realistic for DPSK while still too optimistic for PSK-transmission.

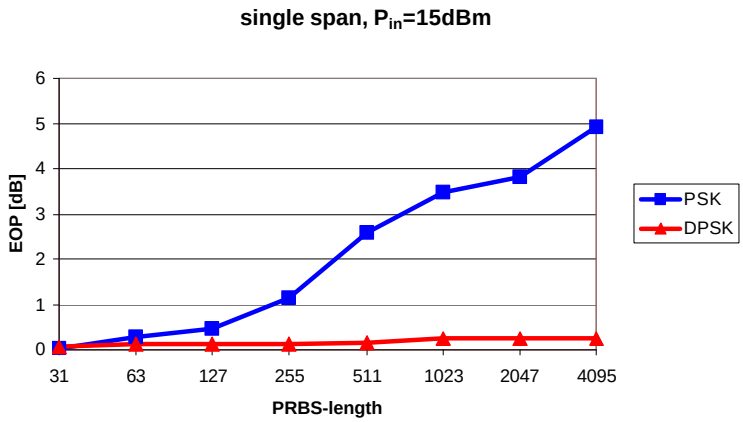

Fig. 4.3: EOP vs. PRBS-length for single span transmission with P_{in}=15dBm for coherent PSK transmission (squares) and self-homodyne DPSK transmission (triangles)

4.4 CF-RZ-DPSK for long-haul transmission

As an example for the excellent properties of self-homodyne DPSK transmission, in fig. 4.4 we present the simulation results for a modulation format we call chirp-free return-to-zero DPSK (CF-RZ-DPSK) in comparison to RZ-ASK. In addition to the transmitter shown in fig. 2.4, a subsequent MZM provides RZ pulse forming. As a consequence, the optical power as a function of time is periodic, which has been shown to further reduce the impact of XPM compared to ASK[6]. As can be seen, even for a relatively high input peak power of 9dBm for each of the eight channels, the EOP after 3000km (30·100km) stays below a level of 1dB compared to RZ-ASK, where an EOP of almost 3dB is obtained.

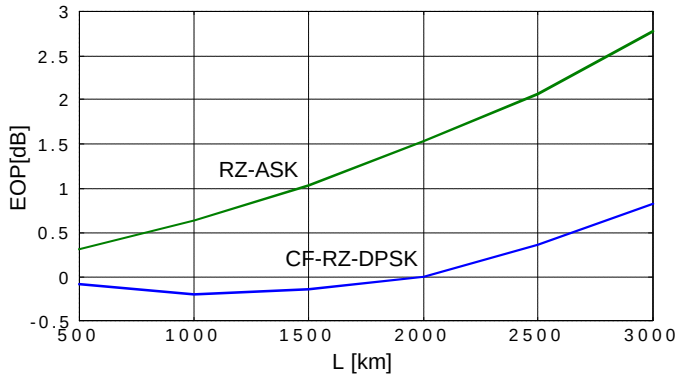

Fig 4.4: 8x10Gb/s with *Df*=100GHz, P_{in} =9dBm/ch: Eye-opening penalty of 4th channel with increasing length

5 CONCLUSION

Starting from classical communications, we have discussed two competing alternatives for the implementation of phase shift keying modulation for optical communications, namely the coherent PSK implementation using a local oscillator and the self-homodyne differential PSK using a delay-and-add demodulator. Although the coherent alternative is known to provide higher receiver sensitivity, the differential implementation is shown to be robust towards cross-phase modulation, one of the most important limiting nonlinear effects for WDM-transmission. On the other hand, coherent PSK is shown to be extremely sensitive towards XPM making transmission of multi-channel WDM nearly impossible.

ACKNOWLEDGEMENT

The authors would like to thank Yuriy Zadoya for helpful discussions.

REFERENCES

1 T.N. Nielsen et al., "3.28Tb/s (82x40Gb/s) transmission over 3x100km nonzero-dispersion fiber using dual C-band and L-band hybrid Raman/Erbium-doped inline amplifiers", *OFC 2000*, paper PD23.

2 K. Fukuchi et al., "10.92-Tb/s (273x40Gb/s) triple-band/ultra-dense WDM optical-repeatered transmission experiment", *OFC 2001*, paper PD24.

3 A.H. Gnauck et al., "2.5Tb/s (64x42.7Gb/s) transmission over 40x100km NZDSF using RZ-DPSK format and all-Raman-amplified spans", *OFC 2002*, paper FC2.

4 W.A. Atia and R.S. Bondurant, "Demonstration of return-to-zero signaling both OOK and DPSK formats to improve receiver sensitivity in an optically preamplified receiver", *IEEE LEOS 1999*, paper TuM3.

5 T. Miyano, M. Fukutoku, K. Hattori, and H. Ono, "Suppression of degradation induced by SPM/XPM+GVD in WDM transmission using a bit-synchronous intensity modulated DPSK signal", *OECC 2000*, paper 14D3-3.

6 J. Leibrich, C. Wree, and W. Rosenkranz, "CF-RZ-DPSK for suppression of XPM on dispersion-managed long-haul optical WDM transmission on standard single-mode fiber", *IEEE Photon. Technol. Lett.* , **14**, no. 2, pp. 155-157, 2002.

7 R.A. Griffin et al., "10Gb/s optical differential quadrature phase shift key (DQPSK) transmission using GaAs/AlGaAs integration", *OFC 2002*, paper FD6.

8 C. Wree, J. Leibrich, and W. Rosenkranz, "RZ-DQPSK format with high spectral efficiency and high robustness towards fiber nonlinearities", *ECOC 2002*, paper 09.6.7

9 S. Norimatsu and K. Iwashita, "The influence of cross-phase modulation on optical FDM PSK homodyne transmission systems", *IEEE J. Lightw. Technol.* , **11**, no. 5/6, pp. 795-804, 1993.

10 M. Rohde et al., "Robustness of DPSK direct detection transmission format in standard fibre WDM systems", *Electron. Lett.* , **36**, pp. 1483-1484, 2000.

11 S. Benedetto and E. Biglieri, *Principles of digital transmission*, Kluwer Academic/Plenum Publishers, New York, 1999.

12 T. Chikama et al., "Modulation and demodulation techniques in optical heterodyne PSK transmission systems", *IEEE J. Lightw. Technol.* , **8**, no. 3, pp. 309-322, 1990.

13 W. Kaiser, T. Wuth, M. Wichers, and W. Rosenkranz, "Reduced complexity optical duobinary 10Gb/s transmitter setup resulting in an increased transmission distance", *IEEE Photon. Technol. Lett.* , **13**, no. 8, pp. 884-886, 2001.

14 D. Marcuse, A.R. Chraplyvy, and R.W. Tkach, "Dependence of cross-phase modulation on channel number in fiber WDM systems", *IEEE J. Lightw. Technol.* , **12**, no. 5, pp. 885-890, 1994.

15 A.V.T. Cartaxo, "Impact of modulation frequency on cross-phase modulation effect in intensity modulation – direct detection WDM systems", *IEEE Photon. Technol. Lett.* , **10**, no. 9, pp. 1268-1270, 1998.

16 G.P. Agrawal, *Nonlinear Fiber Optics*, Academic Press, New York, 1995.

17 N. Sihibata, R.P. Braun, and R.G. Waarts, "Phase-mismatch dependence of efficiency of wave generation through four-wave mixing in a single-mode optical fiber", *IEEE J. Quant. Electron.*, **23**, no. 7, pp. 1205-1210, 1987.

18 T.K. Chiang et al., "Cross-phase modulation in fiber links with multiple optical amplifiers and dispersion compensators", *IEEE J. Lightw. Technol.* , **14**, no. 3, pp. 249-260, 1996.